Renormalization of Coulomb interaction in graphene: Determining observable quantities

Fernando de Juan, Adolfo G. Grushin, and María A. H. Vozmediano
Instituto de Ciencia de Materiales de Madrid, CSIC, Cantoblanco, E-28049 Madrid, Spain
(Received 16 February 2010; revised manuscript received 9 June 2010; published 7 September 2010)

We address the determination of physical observables in graphene in the presence of Coulomb interactions of density-density type modeled with a static Coulomb potential within a quantum field theory perturbative renormalization scheme. We discuss the similarities and differences of the model with quantum electrodynamics and show that all the divergences encountered in the physical quantities are associated to the electron self-energy and can be determined without ambiguities by a proper renormalization of the Fermi velocity and the electron wave function. The renormalization of the photon polarization to second order in perturbation theory—a quantity directly related to the optical conductivity—is given as an example. We also discuss the determination of the effective many-body coupling constant in graphene.

DOI: 10.1103/PhysRevB.82.125409 PACS number(s): 73.22.Pr

I. INTRODUCTION

The role of many-body corrections to the physics of graphene is at this point uncertain. While in the first transport experiments electron-electron interactions seemed not to play a major role[1–3] more recent measurements[4–9] and the observation of the fractional quantum-Hall effect[10,11] indicate the possible importance of the Coulomb interaction to the intrinsic properties of graphene.

The problem of the nature of the interacting system was addressed in detail in the early works on graphene both in the weak[12–15] and in the strong coupling limit.[16–18] The main issue was to determine the infrared nature of the system—its Fermi-liquid character and its associated physical properties. In the weak coupling regime[12] with a perturbative renormalization-group (RG) analysis it was shown that intrinsic graphene behaves as a strange Fermi liquid in the sense that all possible interactions are marginally irrelevant but the inverse electron lifetime grows linearly with the energy instead of quadratically.[13] An upward renormalization of the Fermi velocity at low energies was also predicted what in turn implied a downward renormalization of the effective Coulomb interaction ($g=\frac{e^2}{4\pi\epsilon v}$) to the infrared. Experimental indications of both the linear inverse lifetime of the electron[4,7] and of the Fermi velocity dependence with the energy[9] have been recently reported. The results of these early works have been reproduced and pushed forward under several approaches after the synthesis of graphene.[19–23]

A very important aspect of renormalization was left aside in these previous works: the renormalization of the parameters of the theory that allow to determine the physical observables. The *physical* reality of the cutoff in condensed-matter models has given rise to some confusion in the literature as to whether or not physical observables can depend on the cutoff or on the regularization procedure.[21,22,24,25] We will here follow the standard quantum field theory (QFT) approach to renormalization aiming to give a prescription to calculate unambiguous, cut-off-independent observable results to any order in perturbation theory. We show that all the divergences arising at any order in perturbation theory can be fixed by a proper renormalization of the Fermi velocity and the electron wave-function renormalization. Most of the observables depend exclusively on the Fermi velocity whose value is fixed by an experimental data. We work out as an example the renormalization of the photon self-energy, a quantity directly related to the Coulomb interaction corrections to the optical properties of the system. Although the procedure described in this work follows the standard work done in QFT,[26] some subtleties appear due to the lack of Lorentz covariance and, in some models, of causality which makes this work nontrivial also under a QFT point of view.

II. RENORMALIZATION IN QUANTUM FIELD THEORY

Ultraviolet divergences arise in QFT due to the singular behavior of the fields at very short distances in real space—or at very large energies in Fourier space. Renormalization[26,27] is a prescription to get rid of ultraviolet divergences and construct sensible models where physical quantities can be accurately computed. In renormalizable QFT, one can identify a set of "primitively divergent" Feynman graphs at low order in perturbation theory whose structure coincides with terms existing in the original Lagrangian. All the divergences at higher order can be identified as coming from these previous ones (this will be clarified in what follows). Ultraviolet divergences can be canceled by adding counter terms to the Lagrangian what amounts to a redefinition of the parameters (mass, coupling constant, wave function) of the theory. The process is usually done order by order in perturbation theory. If done appropriately at the end one finds finite results independent of the regularization procedure in the computation of physical observables. The price to pay in this process is the necessity to fix the values of the renormalized parameters at a given energy from some well-chosen experimental inputs. This "renormalization prescription" is crucial in the process and the basis of the later RG developments in QFT.

The determination of the experimental values of the parameters from a given experimental measure often involves phenomenological assumptions. Very good examples of these difficulties are provided by the interplay between the accurate determination of the fine structure constant of QED—that often is done from solid state measurements of

the electron precession in magnetic fields—and its feedback to determine the anomalous magnetic moment of the electron with the actual precision of better than one part in a trillion.[28]

In the condensed-matter applications the difficulty increases due to the fact that we do not have "scattering" experiments involving the asymptotic states of the fields but transport measurements that are influenced by all kinds of extrinsic factors (disorder, doping, or substrate). Yet the renormalization program can be adapted to condensed-matter systems that admit a continuum effective description, graphene being one of the best examples. The independence of the observable quantities on the cutoff guaranteed by the procedure makes it irrelevant whether or not the cutoff has to be taken to infinity or to a finite value defined at high energies as the inverse lattice spacing. It ensures that the observables of the effective low-energy theory do depend on the high energy only through the renormalization of the effective parameters and do not have an explicit dependence on high energy quantities.

Next we will see these words at work in the concrete case of graphene physics. The program consists of identifying the primitively divergent Feynman graphs, adding counterterms to subtract the divergences, redefine the parameters of the model to absorb the infinities, and fix the finite parts of the vertex correlation functions by a renormalization prescription. For this last step we need a number of external conditions (observable data)—the renormalization conditions—equal to the number of parameters to be renormalized. The original RG equations in the QFT approach were established to demonstrate the independence of the observable quantities on the renormalization prescription. Any two set of experimental data will give rise to the same result for a cross section.

III. RENORMALIZATION OF THE GRAPHENE MODEL

A. Definition of the model

A very early tight-binding analysis of the honeycomb lattice[29,30] revealed that the low-energy electronic excitations of a graphene sheet are well described by the massless Dirac Hamiltonian in two space dimensions. This special property arises from the structure of the lattice with two atoms per unit cell and from the very special property that the Fermi level of the neutral system lays at the degenerate points where conduction and valence bands cross. A continuum model arises from the dispersion relation by linearizing the bands around each of the Fermi points. In the clean neutral system at low energies the density of states at the Fermi level vanishes and the Coulomb interactions are unscreened.[12] The noninteracting model considering a single Fermi point is described by the Hamiltonian (in units $\hbar=1$)

$$\mathcal{H}=v_F\int d^2\mathbf{r}\bar{\psi}(\mathbf{r})\gamma^j\partial_i\psi(\mathbf{r}), \tag{1}$$

where $i=1,2$, $\bar{\psi}(\mathbf{r})=\psi^+(\mathbf{r})\gamma^0$, and the gamma matrices can be chosen as $\gamma_x=\sigma_2$, $\gamma_y=-\sigma_1$, $\gamma^0=\sigma_3$. σ_i are the Pauli matrices and v_F is the Fermi velocity (to be defined unambiguously in the next section). The limits of validity of the continuum model of graphene given by the Hamiltonian (1) are twofold: the bending of the bands is neglected what imposes a constraint on the energy E of the processes that can be described: $E\leq 1-1.5$ eV, and a single Fermi point is selected what means that short range disorder or interactions connecting the two Fermi points are neglected. Under these assumptions it was shown in Ref. 31 that the Fermi point is topologically protected and no gap will open from interactions or disorder respecting the symmetries of the system.

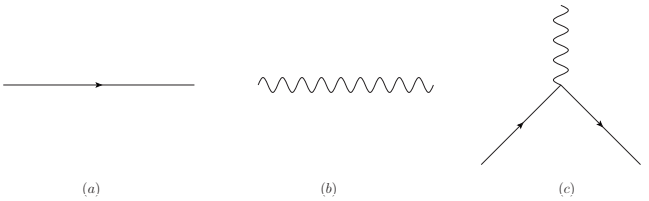

FIG. 1. Tree level Feynman diagrams (see text for details): (a) electron propagator, (b) Photon propagator, and (c) Interaction vertex.

The electron-electron interaction in graphene is described by the Hamiltonian

$$\mathcal{H}_{\text{int}}=e^2\int d^2\mathbf{r}d^2\mathbf{r}'\frac{\psi^+(\mathbf{r})\psi(\mathbf{r})\psi^+(\mathbf{r}')\psi(\mathbf{r}')}{|\mathbf{r}-\mathbf{r}'|}. \tag{2}$$

It is immediately seen that, unlike what happens in the usual two-dimensional electron gas, the ratio of the Coulomb interactions and the kinetic energy in this system is a constant independent of the density and given by $g\sim\frac{e^2}{v_F}$ often taken as the graphene fine structure constant.

We will follow Ref. 14 and model the electron-electron interaction as a density-density interaction mediated by a scalar potential. The (instantaneous) Coulomb interaction can be described by the scalar component of the gauge field

$$\mathcal{H}_{\text{int}}=e\int d^2\mathbf{r}\bar{\psi}(\mathbf{r})\gamma^0\psi(\mathbf{r})A_0(\mathbf{r}) \tag{3}$$

with our choice of gamma matrices.

In order to define the renormalized theory we need a Lagrangian, a renormalization scheme (i.e., a regularization method and a set of renormalization conditions), and the experimentally measured parameters associated with these conditions.

The Lagrangian is

$$\mathcal{L}=\int d^3k[\bar{\psi}(\gamma^0k_0+v\boldsymbol{\gamma}\cdot\mathbf{k})\psi-e\bar{\psi}\gamma^0\psi A_0+A_0|\mathbf{k}|A_0] \tag{4}$$

and it contains four quantities that can be redefined: the velocity v, the parameter e in the interaction, and the electron and gauge field wave functions.

The Feynman rules for the given model are specified by the electron and photon propagators Figs. 1(a) and 1(b) and by the tree level interaction vertex [Fig. 1(c)] $\Gamma^0=-ie\gamma^0$. The electron and photon propagators in momentum space are given by

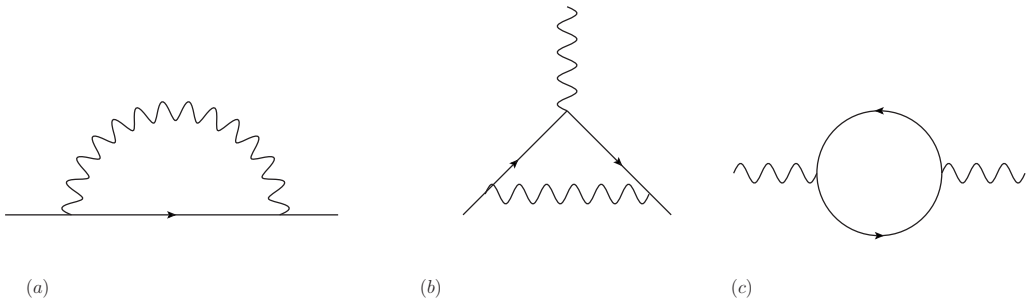

FIG. 2. Primitively divergent Feynman graphs in QED(4).

$$G_0(k^0,\mathbf{k}) = i\frac{\gamma^0 k_0 + v\,\boldsymbol{\gamma}\cdot\mathbf{k}}{-(k^0)^2 + v^2\mathbf{k}^2}, \tag{5}$$

$$\Pi_0(\mathbf{k}) = \frac{1}{2}\frac{1}{|\mathbf{k}|}. \tag{6}$$

The standard Coulomb interaction in Eq. (2) can be recovered from Eq. (4).

The model was shown to be gauge invariant and renormalizable in Ref. 12. The renormalization functions can be defined from the self-energy and the vertex as

$$G_0^{-1} - \Sigma(k^0,\mathbf{k}) = Z_\psi^{1/2}(k^0,\mathbf{k})[k^0\gamma^0 - Z_v(k^0,\mathbf{k})v\,\boldsymbol{\gamma}\cdot\mathbf{k}], \tag{7}$$

$$\Gamma = Z_e e\,\gamma^0. \tag{8}$$

It is important to note that when renormalizing at a given order in perturbation theory, the vertex functions (amputated one particle irreducible Green's functions) directly related to the observable quantities have to be computed as a sum of all the corrections and counterterms up to this order. It does not make sense to renormalize a single diagram.

An RG analysis of the model (1) shows that four Fermi or other local interactions are irrelevant while Coulomb interactions modeled by coupling the electronic current $J^\mu(x) = \bar{\Psi}(x)\gamma^\mu\Psi(x)$ to a vector field A_μ with a $(1/r)$ propagator are marginal.

B. Renormalization of the model. Graphene versus QED

In QED(3+1) there are three primitive divergent diagrams shown in Fig. 2 and three free parameters in the model: the electron and photon wave functions, and the coupling constant. The model is strictly renormalizable and when computing a higher loop diagram we get higher powers of the logarithmic divergence. The renormalization of the fine structure constant $\alpha_{\mathrm{QED}} = \frac{e^2}{4\pi c}$ is due to the charge renormalization coming from the photon self-energy. The electron wave-function renormalization (there is no velocity parameter there) gives rise to an anomalous dimension. As it is known, the coupling constant (electric charge) renormalizes to zero in the infrared and the theory is infrared free. QED(2+1) is different. There, the coupling constant has a positive dimension of mass $(\sqrt{M})$ and the theory is called "superrenormalizable." It means that it has less divergences than its four-dimensional counterpart. In fact, there are no ultraviolet infinities in QED(2+1). The massless theory has infrared divergences that can also be cured.[32]

The graphene model stands in between the two QED cases due to the anomalous gauge propagator chosen. In QFT a gauge field (in general, any vector field) has a kinetic term with two derivatives and hence a $1/k^2$ propagator in any number of dimensions. When Fourier transformed it gives rise to a $1/r$ interaction in four dimensions and a logarithmic interaction in planar models (2+1). In the graphene model the gauge field propagator has a $(1/k)$ dependence. The reason is that, although the electrons are confined to the two dimensional plane, the electromagnetic field lives in three spatial dimensions. This makes the interaction term in the Lagrangian scale invariant (critical point) what has interesting consequences[33,34] and in this respects it resembles QED(4) rather than QED(3). This is also what induces a renormalization of the electron self-energy not present in QED(3). In what follows we will see that all the infinities of the model are related to the electron self-energy which renormalizes the Fermi velocity at the one loop level and the wave function at higher orders.

In the model defined by Eq. (4) the only primitively divergent graph at the one loop level is the one corresponding to the electron self-energy in Fig. 2(a) and of this, the divergence only affects the spatial part of the momentum. The result of the computation of the diagram with a hard cutoff is

$$\Sigma_\Lambda^{(1)}(\mathbf{k}) = -\frac{g}{4}v\,\boldsymbol{\gamma}\cdot\mathbf{k}\left(-\log\frac{\mathbf{k}^2}{\Lambda^2} + 4\,\log 2\right). \tag{9}$$

The electron self-energy can be made finite at this order in perturbation theory by including at tree level a counterterm of the form depicted in Fig. 3 with the associated Feynman rule

$$\Sigma_{ct,\Lambda}^{(1)}(\mathbf{k}) = \frac{g}{4}v\,\boldsymbol{\gamma}\cdot\mathbf{k}(\log\,\Lambda^2 + 4\,\log 2 + F_\Lambda). \tag{10}$$

As expected in a renormalizable theory, the counterterm has the same operator dependence as a term in the original

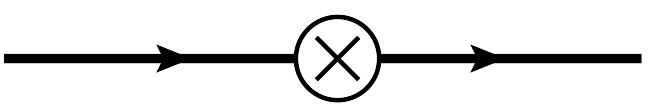

FIG. 3. Tree level counterterm associated to the electron self-energy. See text for details.

Lagrangian. Since the only requirement to impose on it is to cancel the divergent part of the given diagram it contains a momentum-independent arbitrary finite part F_Λ to be fixed by the renormalization condition, i.e., by an experimental measure that allows to extract the value of the two point function at a given momentum k_R. This condition introduces the scale that settles the apparent dimensional mismatch in Eq. (10). The calculation in a dimensional regularization scheme follows exactly the same steps with an equivalent finite arbitrary part in the counterterm F_μ instead of F_Λ which is eliminated by the renormalization condition. That the procedure of renormalization does not depend on the cutoff is obvious considering that there exists a renormalization procedure (BPHZ scheme) that does not require the use any cutoff.[26]

Notice that although being a tree level interaction, the counterterm in Eq. (10) is of order g. This diagram has to be added in the construction of the vertex functions at each given order in perturbation theory. In particular, it will affect the photon polarization at second order discussed in Sec. III D.

Summing up the contributions of the tree level plus the two Feynman graphs of order g [Figs. 2(a) and 3] the two-point function is

$$G_\Lambda^{-1}(k^0,\mathbf{k}) = -i\left(\gamma^0 k_0 + v\boldsymbol{\gamma}\cdot\mathbf{k}\left[1-\frac{g}{4}(\log\mathbf{k}^2+F_\Lambda)\right]\right) \tag{11}$$

that can be written as

$$G_\Lambda^{-1}(k^0,\mathbf{k}) = -i[\gamma^0 k_0 + v(\mathbf{k})\boldsymbol{\gamma}\cdot\mathbf{k}] \tag{12}$$

with

$$v(\mathbf{k}) = v\left[1-\frac{g}{4}(\log\mathbf{k}^2+F_\Lambda)\right]. \tag{13}$$

The two-point function in Eq. (12) has the same form as the free one with a k-dependent and arbitrary parameter $v(\mathbf{k})$. The last step of the renormalization program is to fix the arbitrariness with a renormalization condition. For this we need an experimental measure of the Fermi velocity at a given value of the momentum k_R as it will be discussed in the next section.

This finishes the renormalization of the theory to first order in perturbation theory (one loop level). Any observable quantity at this level can be computed with the Feynman diagrams of Figs. 1 and 3 and will be finite and independent of the regularization procedure.

C. Determining the Fermi velocity and the coupling constant

The experimental determination of the Fermi velocity of graphene[35] is an important and elusive issue similar to the determination of the fine structure constant in QED(3+1) and we will discuss this further in the discussion section. This is almost the only parameter in the theory and it enters into practically all observable quantities. The fact that it can vary as a function of the energy or even of the position on the sample[36] must be taken into account for the correct interpretation of the experimental results.

As in the precision tests of QED, each comparison between theory and experiment can be seen as an independent determination of v_F. To exemplify how the renormalization works we can take as an example the experimental value of the Fermi velocity given in Ref. 37.

$$v(125\ \text{meV}) = 1.093\times 10^6\ \text{m/s} \equiv v_F. \tag{14}$$

With this condition we fix the value of F_Λ choosing the bare velocity to be $v=v_F$. The physical Fermi velocity will depend on the energy at which it is measured and on the renormalization point k_R (125 meV in this case) which becomes a part of the defining theory:

$$v_R(\mathbf{k}) = v_F\left[1-\frac{g}{4}\log\left(\frac{\mathbf{k}^2}{\mathbf{k}_\mathbf{R}^2}\right)\right]. \tag{15}$$

The definition of the running velocity defines the running coupling constant

$$g_R(\mathbf{k}) = \frac{e^2}{4\pi v_R(\mathbf{k})}. \tag{16}$$

Two different renormalization prescriptions for the Fermi velocity measured at points k_A, k_B are related by the renormalization-group equation

$$\frac{v(\mathbf{k}_A)}{v(\mathbf{k}_B)} = 1-\frac{g_B}{4}\log\left(\frac{\mathbf{k}_A}{\mathbf{k}_B}\right), \tag{17}$$

where g_B is the coupling at momentum k_B. Hence, it is the RG that ensures that the exact theory is independent of the experimental point chosen in Eq. (14). This in turn guarantees the consistency of the renormalization procedure.

Another important issue which has been overlooked in previous works concerns the determination of the effective coupling constant of the many-body interactions in graphene. This quantity is usually defined as a function of the Fermi velocity as $g=\frac{e^2}{4\pi\epsilon v_F}$, where ϵ is the dielectric constant of the substrate. It is assumed that e is the bare charge of the electrons. From the point of view of defining a sensible model to compute observables the dielectric constant is an external constraint that cannot be controlled. The parameter e nevertheless is a free parameter in the Lagrangian that is not renormalized. As such its precise value has to be determined with yet another independent experiment and there are no *a priori* reasons to assume the naked value. The expression (17) can be used to find the precise value of e if the Fermi velocity can be accurately measured at two different close energies E_A, E_B near the Dirac point in the suspended very clean samples recently available. Since at the suspended samples $\epsilon=1$ we will have for, say, $E_B\sim 2E_A$, $\frac{e^2}{4\pi}\sim(v_A-v_B)$.

D. Photon propagator. Optical conductivity

As happens in QED(2+1), the photon propagator depicted in Fig. 2(b) is finite at the one loop level. This one loop result is independent on the nature of the interaction since only electron propagators appear in the calculation. Different interaction vertices describing Yukawa couplings, scalar potentials, or disorder couplings may change the ten-

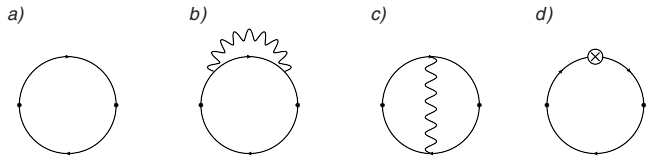

FIG. 4. Feynman diagrams contributing to the photon self-energy to second order in perturbation theory.

sor structure but the diagram will remain finite. In QED(3+1) this diagram has a logarithmic singularity and the photon polarization has higher powers of logs at higher orders in perturbation theory what gives rise to the electric charge renormalization. A related issue is that at this order in perturbation theory there are no Coulomb interaction corrections to the optical conductivity of the system. As it is clear from our analysis any correction appearing at higher orders in perturbation theory will originate in subdivergences related to the primitively divergent graph of Fig. 2(a). Vertex-type corrections as the one depicted in Fig. 4(c) will be finite at all orders in the present model. The full photon propagator at order g^2 will be given by the sum of the diagrams shown in Fig. 4. Diagrams Figs. 4(a) and 4(c) are finite in this model.

The diagram in Fig. 4(b) contains a sub divergent diagram which is identified as the first order correction to the electron self-energy diagram discussed in the previous section. This divergence is canceled by the diagram in Fig. 4(d) leaving a finite, unambiguous, result.

The sum of diagrams 4(b) and 4(d) reads

$$\Pi_b + \Pi_d = -e^2 \int \frac{d^3k}{(2\pi)^3} \gamma^0 G(k) \times \left[\Sigma_{ct}^{(1)} - ie^2 \int \frac{d^3p}{(2\pi)^3} \gamma^0 G \times (k+p)\gamma^0 \frac{1}{|\mathbf{p}|} \right] G(k)\gamma^0 G(k+q), \tag{18}$$

where $\Sigma_{ct}^{(1)}$ is given by Eq. (10). We can identify the piece in the brackets as the renormalized electron self-energy with both contributions from the diagram in Fig. 2(a) and its counterterm shown in Fig. 3. Hence the inner loop has already been computed and the potentially divergent part that remains is

$$\Pi_b + \Pi_d \sim \frac{e^4}{32\pi v_F} \int \frac{d^3k}{(2\pi)^3} \mathrm{Tr} \frac{\gamma^0(\gamma^0 k_0 + v_F \boldsymbol{\gamma}\cdot\mathbf{k})\boldsymbol{\gamma}\cdot\mathbf{k}(\gamma^0 k_0 + v_F \boldsymbol{\gamma}\cdot\mathbf{k})\gamma^0[\gamma^0(k_0+q_0) + v_F \boldsymbol{\gamma}\cdot(\mathbf{k}+\mathbf{q})]\log\frac{\mathbf{k}^2}{\mathbf{k}_R^2}}{(-k_0^2 + v_F^2\mathbf{k}^2)^2[-(k_0+q_0)^2 + v_F^2(\mathbf{k}+\mathbf{q})^2]}. \tag{19}$$

We have computed explicitly this contribution in both dimensional regularization and a hard cutoff and it is finite and independent on the regularization procedure. Thus, the renormalization procedure for the photon propagator is complete to second order in perturbation theory by means of the renormalization condition that made the electron propagator finite to first order in perturbation theory.

Most of the electromagnetic response properties of the system are given by the photon propagator. The complex dielectric function $\epsilon(\omega,\mathbf{q})$ is defined as

$$\frac{1}{\epsilon(\mathbf{q},\omega)} = 1 + V_0(\mathbf{q})\Pi(\mathbf{q},\omega). \tag{20}$$

In the limit $\omega \to 0$ it gives the static screening properties of the system and is purely real. In undoped graphene no finite screening length is generated and the effective Coulomb potential remains long ranged. The conductivity can also be obtained as

$$\sigma(\omega) = \lim_{\mathbf{q}\to 0} \frac{i\omega}{q^2}\Pi(\mathbf{q},\omega). \tag{21}$$

The optical conductivity can be computed from Eq. (21). The zeroth-order dynamical conductivity comes from the one-loop diagram in Fig. 4(a) which gives the well known expression

$$\sigma_0(\omega) = \frac{\pi}{2}\frac{e^2}{h} \tag{22}$$

independent of the energy. The Coulomb interaction corrections to the optical conductivity can be obtained from the photon propagator at second order in perturbation theory discussed above. Since we have not computed the finite parts of the diagrams involved we cannot give a precise number but from this discussion it is clear that the result does not depend on the regularization prescription and it only depends on the chosen experimental data fixing the Fermi velocity.

In the particular case of the real part of the conductivity to two loops order,[22,24,25] the inclusion of counterterms does not produce any change in the computation, other than the fact that the renormalized coupling constant must be used. But the use of a renormalized theory will be essential to ensure cut-off independence in the computation of the imaginary part, the **q**-dependent dielectric function, or higher orders in the real part.

IV. CONCLUSIONS AND DISCUSSION

In this work we have addressed the determination of physical observables in graphene in the presence of Coulomb interactions of density-density type modeled with a static

Coulomb potential within a QFT perturbative renormalization scheme. We have shown that all the divergences up to two loops of the physical quantities are associated to the one loop electron self-energy and can be regulated by a proper renormalization of the Fermi velocity. The consistency of the scheme presented was exemplified by the renormalization of the photon polarization at the two loops level. We have shown that the Coulomb interaction corrections to the optical conductivity are fixed unambiguously with a proper renormalization of the Fermi velocity and do not depend on the regularization scheme.

The QFT renormalization procedure outlined in this work shows that it can also be applied to condensed-matter theories where there is an ultraviolet physical cutoff (the inverse of the lattice spacing $\Lambda \sim 1/a$) that prevents the appearance of infinities. Although initially devised to get rid of ultraviolet divergences, the QFT renormalization in more modern approaches is a way to define the physical parameters of effective theories in a given range of energies that do not depend on the details or parameters at higher energies.

As we have seen the most important parameter in the computation of the observable quantities in graphene is the renormalized Fermi velocity that defines the Coulomb coupling constant. In the model discussed in this work the Fermi velocity grows without bound in the infrared.[12] This sets a lower bound on the validity of the model that breaks down when the Fermi velocity approaches the speed of light c. The scale defines an infrared cutoff δ for the theory and can be computed as

$$\delta = k_R \exp\left\{ -\frac{16\pi[c - v(k_R)]}{e^2} \right\}. \tag{23}$$

This estimate depends on the renormalization point k_R and on $v(k_R)$. Plugging in the measured values we realize that the huge exponential suppression gives an infrared cutoff below any experimental resolution. This does not impose any real bound on the validity of the model from an experimental point of view. The limits of validity of the static model are set by internal consistency of the theory: the choice of a charge-charge interaction made to model Coulomb interactions is consistent with the static approximation since both are related to the ratio of Fermi velocity over the speed of light. When the Fermi velocity increases it would be more consistent to consider a retarded Coulomb interaction and a full interaction vertex. The retarded model was analyzed up to one loop in Ref. 12 and has been revised recently in Ref. 38.

For the renormalization procedure to be complete, the fine structure constant of graphene $g = \frac{e^2}{4\pi\epsilon v_F}$ must be fixed, being an important quantity that appears in all the electronic properties of the system. A precise experimental determination is a necessity as the experiments in graphene are reaching a high degree of accuracy. The program to fix this constant can be similar to the one followed in the case of the electromagnetic fine structure constant.[28] In the case of graphene the theoretical determination is much simpler since there are no mass parameters relations involved in the calculations. Moreover it is very interesting the additional fact that the quantity determining α_G (Fermi velocity) is by itself an observable related to the one particle properties of the system. We expect that a proper combination of photoemission[5,39] optical[8] and transport[7,40] measures with the corresponding calculations in the renormalization scheme described here should be enough to determine g as precisely as needed both theoretically and experimentally as it happens in QED $(3+1)$. As discussed in this work, an independent experimental measurement is needed also to fix the value of e, a free parameter in the Lagrangian.

The renormalization program described in this work can be carried out to all orders in perturbation theory. As described in Refs. 12 and 14, the electron self-energy at the two loops level has a logarithmic singularity that induces a wave-function renormalization. A new counterterm of order g^2 has to be added that affects the photon polarization function at the three loops level. This counterterm can be fixed by the same renormalization condition used to fix the Fermi velocity: requiring that the two point function at the two loops order has the same form as the free one, with a finite residue at k_R given by a second experimental input. In the present model all physical quantities are fixed by renormalizing the electron propagator only. It is worth noticing that with the instantaneous Coulomb interaction discussed in this work, the wave-function renormalization does not give rise to an anomalous exponent and the residue of the quasiparticle in the random phase approximation done in Ref. 14 is finite at the Fermi surface implying that, despite the anomalous lifetime[13] the system is closer to a Fermi liquid than to a marginal Fermi liquid.[41]

ACKNOWLEDGMENTS

M.A.H.V. thanks A. González-Arroyo for enjoyable discussions on renormalization in Quantum Field Theory and A. Geim for discussing the experimental possibilities of observing the renormalization of the Fermi velocity. Support by MEC (Spain) under Grant No. FIS2008-00124 is acknowledged.

[1] K. S. Novoselov, A. K. Geim, S. V. Morozov, D. Jiang, Y. Zhang, S. V. Dubonos, I. V. Gregorieva, and A. A. Firsov, Science **306**, 666 (2004).

[2] K. S. Novoselov, A. K. Geim, S. V. Morozov, D. Jiang, M. I. Katsnelson, I. V. Grigorieva, S. V. Dubonos, and A. A. Firsov, Nature (London) **438**, 197 (2005).

[3] Y. Zhang, Y.-W. Tan, H. L. Stormer, and P. Kim, Nature (London) **438**, 201 (2005).

[4] Z. Jiang, E. A. Henriksen, L. C. Tung, Y.-J. Wang, M. E. Schwartz, M. Y. Han, P. Kim, and H. L. Stormer, Phys. Rev. Lett. **98**, 197403 (2007).
[5] A. Bostwick, T. Ohta, T. Seyller, K. Horn, and E. Rotenberg, Nat. Phys. **3**, 36 (2007).
[6] S. Y. Zhou, D. A. Siegel, A. V. Fedorov, and A. Lanzara, Phys. Rev. B **78**, 193404 (2008).
[7] G. Li, A. Luican, and E. Y. Andrei, Phys. Rev. Lett. **102**, 176804 (2009).
[8] R. Nair, P. Blake, A. Grigorenko, K. Novoselov, T. Booth, T. Stauber, N. Peres, and A. Geim, Science **320**, 1308 (2008).
[9] Z. Q. Li, E. A. Henriksenand, Z. Jiang, Z. Ha, M. C. Martin, P. Kim, H. L. Stormer, and D. N. Basov, Nat. Phys. **4**, 532 (2008).
[10] X. Du, I. Skachko, F. Duerr, A. Luican, and E. Andrei, Nature (London) **462**, 192 (2009).
[11] K. I. Bolotin, F. Ghahari, M. D. Shulman, H. L. Stormer, and P. Kim, Nature (London) **462**, 196 (2009).
[12] J. González, F. Guinea, and M. A. H. Vozmediano, Nucl. Phys. B **424**, 595 (1994).
[13] J. González, F. Guinea, and M. A. H. Vozmediano, Phys. Rev. Lett. **77**, 3589 (1996).
[14] J. González, F. Guinea, and M. A. H. Vozmediano, Phys. Rev. B **59**, R2474 (1999).
[15] J. González, F. Guinea, and M. A. H. Vozmediano, Phys. Rev. B **63**, 134421 (2001).
[16] D. V. Khveshchenko, Phys. Rev. Lett. **87**, 246802 (2001).
[17] D. V. Khveshchenko, Phys. Rev. Lett. **87**, 206401 (2001).
[18] E. V. Gorbar, V. P. Gusynin, V. A. Miransky, and I. A. Shovkovy, Phys. Rev. B **66**, 045108 (2002).
[19] S. Das Sarma, E. H. Hwang, and W.-K. Tse, Phys. Rev. B **75**, 121406(R) (2007).
[20] Y. Barlas, T. Pereg-Barnea, M. Polini, R. Asgari, and A. H. MacDonald, Phys. Rev. Lett. **98**, 236601 (2007).
[21] E. G. Mishchenko, Phys. Rev. Lett. **98**, 216801 (2007).
[22] E. G. Mishchenko, EPL **83**, 17005 (2008).
[23] V. N. Kotov, B. Uchoa, and A. H. Castro Neto, Phys. Rev. B **78**, 035119 (2008).
[24] I. F. Herbut, V. Juricic, and O. Vafek, Phys. Rev. Lett. **100**, 046403 (2008).
[25] D. E. Sheehy and J. Schmalian, Phys. Rev. B **80**, 193411 (2009).
[26] J. Collins, *Renormalization* (Cambridge University Press, Cambridge, 1984).
[27] C. Nash, *Relativistic Quantum Fields* (Academic Press, New York, 1978).
[28] D. Hanneke, S. Fogwell, and G. Gabrielse, Phys. Rev. Lett. **100**, 120801 (2008).
[29] P. R. Wallace, Phys. Rev. **71**, 622 (1947).
[30] J. C. Slonczewski and P. R. Weiss, Phys. Rev. **109**, 272 (1958).
[31] J. L. Mañes, F. Guinea, and M. A. H. Vozmediano, Phys. Rev. B **75**, 155424 (2007).
[32] R. Jackiw and S. Templeton, Phys. Rev. D **23**, 2291 (1981).
[33] D. E. Sheehy and J. Schmalian, Phys. Rev. Lett. **99**, 226803 (2007).
[34] J. Wang, H. A. Fertig, and G. Murthy, Phys. Rev. Lett. **104**, 186401 (2010).
[35] A. K. Geim, Science **324**, 1530 (2009).
[36] F. de Juan, A. Cortijo, and M. A. H. Vozmediano, Phys. Rev. B **76**, 165409 (2007).
[37] R. S. Deacon, K.-C. Chuang, R. J. Nicholas, K. S. Novoselov, and A. K. Geim, Phys. Rev. B **76**, 081406(R) (2007).
[38] A. Giuliani, V. Mastropietro, and M. Porta, arXiv:1001.5347 (unpublished).
[39] S. Zhou, G.-H. Gweon, J. Graf, A. Fedorov, C. Spataru, R. Diehl, Y. Kopelevich, D.-H. Lee, S. G. Louie, and A. Lanzara, Nat. Phys. **2**, 595 (2006).
[40] X. Du, I. Skachko, A. Barker, and E. Y. Andrei, Nat. Nanotechnol. **3**, 491 (2008).
[41] C. M. Varma, P. B. Littlewood, S. Schmitt-Rink, E. Abrahams, and A. E. Ruckenstein, Phys. Rev. Lett. **63**, 1996 (1989).